Clinical and Experimental Immunology, 2023, **211**, 57–67
https://doi.org/10.1093/cei/uxac120
Advance access publication 26 December 2022
Research Article

Research Article

miR-132-3p regulates antibody-mediated complement-dependent cytotoxicity in colon cancer cells by directly targeting CD55

Yu Fan, Juan Liao, Yu Wang, Zhu Wang, Hong Zheng and Yanping Wang*

Multi-omics Laboratory of Breast Diseases, West China Hospital, Sichuan University, Chengdu, Sichuan, China

*Correspondence: Yanping Wang, 5# Gongxing Street, Chengdu, Sichuan, China. Email: wyanping@scu.edu.cn

Abstract

The overexpression of membrane-bound complement regulatory proteins (mCRPs) on tumour cells helps them survive complement attacks by suppressing antibody-mediated complement-dependent cytotoxicity (CDC). Consequently, mCRP overexpression limits monoclonal antibody drug immune efficacy. CD55, an mCRP, plays an important role in inhibiting antibody-mediated CDC. However, the mechanisms regulating CD55 expression in tumour cells remain unclear. Here, the aim was to explore CD55-targeting miRNAs. We previously constructed an *in vitro* model comprising cancer cell lines expressing α-gal and serum containing natural antibodies against α-gal and complement. This was used to simulate antibody-mediated CDC in colon cancer cells. We screened microRNAs that directly target CD55 using LoVo and Ls-174T colon cell lines, which express CD55 at low and high levels, respectively. miR-132-3p expression was dramatically lower in Ls-174T cells than in LoVo cells. miR-132-3p overexpression or inhibition transcriptionally regulated *CD55* expression by specifically targeting its mRNA 3′-untranslated regions. Further, miR-132-3p modulation regulated colon cancer cell sensitivity to antibody-mediated CDC through C5a release and C5b-9 deposition. Moreover, miR-132-3p expression was significantly reduced, whereas CD55 expression was increased, in colon cancer tissues compared to levels in adjacent normal tissues. CD55 protein levels were negatively correlated with miR-132-3p expression in colon cancer tissues. Our results indicate that miR-132-3p regulates colon cancer cell sensitivity to antibody-mediated CDC by directly targeting CD55. In addition, incubating the LoVo human tumour cell line, stably transfected with the xenoantigen α-gal, with human serum containing natural antibodies comprises a stable and cheap *in vitro* model to explore the mechanisms underlying antibody-mediated CDC.

Graphical abstract

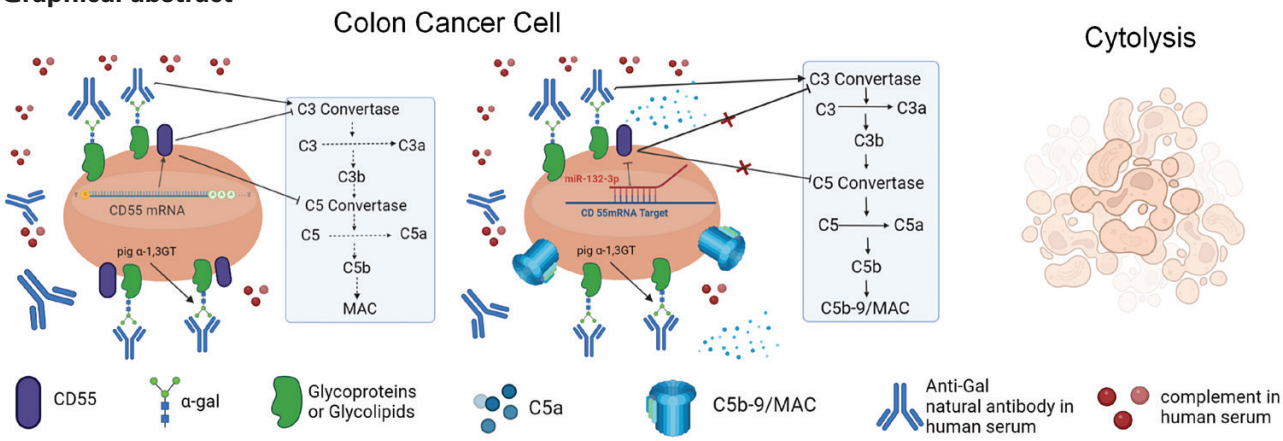

Keywords: miR-132-3p, CD55, antibodies, complement-dependent cytotoxicity, colon cancer

Abbreviations: 3′-UTRs: 3′-untranslated regions; BMI: Banna minipig inbred-line; BSA: bovine serum albumin; CDC: complement-dependent cytotoxicity; H&E: haematoxylin and eosin; IHC: immunohistochemistry; INHS: heat-inactivated pooled normal human serum; mAbs: monoclonal antibodies; MAC: membrane attack complex; mCRPs: membrane-bound complement regulatory proteins; miRNAs: microRNAs; miR-NC: control miRNA; NHS: normal human serum; pTNM: tumour size, lymph node involvement, and the distant metastasis; α-1,3GT: α-(1,3)-galactosyltransferase; α-gal: Gala1-3Galb1-4GlcNAc-R.

Received 19 May 2022; Revised 18 October 2022; Accepted for publication 22 December 2022

Introduction

Therapeutic anti-tumour monoclonal antibodies (mAbs), such as CD20-targeting rituximab, CD52-targeting alemtuzumab, Her2-targeting pertuzumab and trastuzumab, and EGFR-targeting cetuximab, which target surface antigens expressed on tumour cells, have been widely used for the treatment of cancer [1, 2]. Despite their remarkable clinical success, some patients do not benefit from these treatments because of intrinsic or acquired resistance. The most important molecular mechanisms underlying the anti-tumour effects of mAbs include the targeted inhibition of signalling pathways, such as growth factor receptors or angiogenesis pathways, which suppress downstream signalling and lead to apoptosis [3, 4]. In addition, mAbs can trigger an innate immune response to induce immune-mediated cell destruction mediated by antibody-dependent cell-mediated cytotoxicity, complement-dependent cytotoxicity (CDC), and antibody-dependent cell-mediated phagocytosis [5–7]. Therefore, enhancing immune-mediated cell destruction is a promising strategy to improve the clinical efficacy of mAbs.

CDC is one of the mechanisms by which antibodies can induce specific target cell lysis through activation of the complement system. To maintain body homeostasis, complement activation is controlled by multiple factors [8], such as membrane-bound complement regulatory proteins (mCRPs), including CD55, CD59, CD46, and CD35 [9, 10]. Many tumour cells overexpress at least one mCRP to evade mAb-mediated CDC [11]. Therefore, inhibiting the expression of one or more of these proteins might reactivate the CDC pathway in some mCRP-highly expressing cancer cells and enhance cell lysis mediated by antibody drugs. Our previous study found that CD55 and CD59 are important inhibitors of trastuzumab-induced cytolysis in breast cancer, and their expression was determined to be correlated with resistance to mAbs and the risk of relapse [12]. More importantly, CD55 overexpression is an independent risk factor for recurrence in breast cancer patients who received postoperative adjuvant trastuzumab therapy [13].

The carbohydrate epitope Gala1-3Galb1-4GlcNAc-R (α-gal) is a heterologous xenoantigen that causes hyperacute rejection. It is widely present in new world monkeys and non-primate mammalian species, but not in humans because the α-(1,3)-galactosyltransferase (α-1,3GT) that catalyses the synthesis of α-gal was inactivated during evolution [13–15]. The incubation of the cancer cells engineered to express the α-1,3GT gene with human serum, containing abundant naturally existing anti-α-gal epitope antibodies, results in immediate initiation of the complement system through the classical pathway and the subsequent lysis of tumour cells due to CDC. This process is in accordance with mAb-mediated CDC [16, 17]. We previously established a stable α-gal-expressing colon cancer cell model and found that its sensitivity to α-gal-mediated CDC is related to the expression level of CD55 [18]. Therefore, we showed that using cancer cell lines expressing low levels of CD55 and engineered to express the α-1,3GT or α-gal gene is not only a possible strategy for anti-tumour therapy research but also a stable and effective cell model to explore regulators affecting Ab-mediated CDC. However, the mechanisms underlying the regulation of CD55 expression in tumour cells remain largely unknown.

MicroRNAs (miRNAs) are highly conserved endogenous non-coding RNAs of ~20–22 nucleotides. They inhibit the expression of targeted genes by targeting mRNAs for cleavage or translational repression via complementary base-pairing with the 3′-untranslated regions (3′-UTRs) of target gene mRNAs [19, 20]. Recent studies have indicated that miRNAs play functional roles in complement-mediated tumour immune escape and can directly or indirectly target mCRPs and affect complement attacks on cancer cells [21–23]. Although many databases and target prediction tools have been used to identify potential CD55-targeting miRNAs [24], identifying the true target proteins, and pathophysiological processes regulated by miRNAs remains challenging.

In this study, we explored the miRNAs that target CD55 by comparing miRNA expression patterns between colon cancer cell lines with high and low CD55 expression. We found that miR-132-3p directly targets the 3′-UTR of *CD55* and post-transcriptionally suppresses its expression. miR-132-3p mimics were found to promote α-gal-mediated complement activation and enhance antibody-mediated CDC in colon cancer cells. In colon cancer tissues, low miR-132-3p expression was correlated with high CD55 expression. Therefore, miR-132-3p might be a promising therapeutic target to reverse the inhibition of CDC caused by the increased expression of CD55 and ultimately improve the efficacy of antibody drugs.

Methods

Cell lines and cell culture

Human LoVo and Ls-174T colonic adenocarcinoma cells and the HEK-293T embryonic kidney cell line were purchased from the Type Culture Collection of the Chinese Academy of Sciences, Shanghai, China. In our previous study, stable LoVo-GT and Ls-174T-GT α-gal-expressing cell lines were obtained by engineering them to express the Banna minipig inbred-line (BMI) α-1,3GT gene [18]. All cells were cultured in RPMI-1640 (Hyclone, Waltham, MA, USA) supplemented with penicillin/streptomycin and 10% foetal bovine serum in a humidified incubator with 5% CO_2 at 37°C, according to the recommended culture method. An appropriate concentration of geneticin (G418) was added to the medium of LoVo-GT and Ls-174T-GT cells at regular intervals to maintain the stable expression of α-gal. The expression of α-gal on the membrane of stable cell populations was detected using fluorescein isothiocyanate FITC-conjugated *Griffonia simplicifolia* isolectin B4 (FITC-BS-IB4 lectin; Vector, Miami, FL), which specifically binds α-gal.

Sera

We recruited 10 staff in our lab to donate whole blood (10 ml from each) and isolate the serum. Pooled normal human serum (NHS) was used as the source of both complement- and anti-α-gal-specific antibodies. NHS was stored at −80°C in aliquots until it was assayed. Heat-inactivated pooled normal human serum (INHS) was prepared by heating NHS to 56°C for 30 min.

Human tissue specimens

Twenty colon tumour tissue specimens and normal adjacent non-tumour tissue specimens were retrospectively collected from the Biobank of the West China Hospital, Sichuan University. Tissues were flash-frozen after surgery. The tumours were staged according to the tumour size, lymph

node involvement, and the distant metastasis (pTNM) classification system. A summary of the tumour sample characteristics is presented in Supplementary Table 1. The expression levels of miR-132-3p and CD55 in the tumours and in the paired normal tissue were tested by RT-qPCR and immunohistochemistry (IHC), respectively.

miRNA transfection

miR-132-3p mimics and the inhibitor, as well as miR-NC mimics and the inhibitor, were purchased from GenePharma (Shanghai, China). Cells were transfected with these oligonucleotides using Lipofectamine 2000 and Opti-MEM I transfection medium (Invitrogen, Carlsbad, CA, USA) according to the manufacturer's instructions. The sequences of the RNA oligonucleotides were as follows: for miR-132-3p mimics, sense: 5′-UAACAGUCUACAGCCAUGGUCG-3′, anti-sense: 5′-ACCAUGGCUGUAGACUGUUAUU-3′; for the miR-132-3p inhibitor, sense: 5′-CGACCAUGGCUGUAGACUGUUA-3′; for the negative control, sense: 5′-UUCUCCGAACGUGUCACGUTT-3′, anti-sense: 5′-ACGUGACACGUUCGGAGAATT-3′; for the inhibitor negative control, sense: 5′-CAGUACUUUUGUGUAGUACAA-3′.

RNA extraction and RT-qPCR

Total RNA, including miRNAs, was extracted from cancer cells using the Total RNA kit (Omega Bio-Tek, China) or isolated from clinical specimens using TRIzol reagent (Invitrogen, Carlsbad, CA, USA), after which RT-qPCR was used to quantify *CD55* mRNA and miRNA expression. First-strand cDNA was synthesized from total RNA, performed using the All-in-one TM miRNA First-Strand cDNA Synthesis Kit (GeneCopoeia, Rockville, MD, USA), and PCR amplification was carried out using the All-in-oneTM miRNA RT-qPCR Detection Kit (GeneCopoeia, Rockville, MD, USA) with the following thermal cycling conditions: 95°C for 10 min; 40 cycles of 95°C for 10 s, 55°C for 20 s, and 72°C for 30 s. To detect miRNA expression, non-coding small nuclear RNA (U6) was used as the internal control.

For *CD55* mRNA, first-strand cDNA was synthesized using the iScript cDNA Synthesis Kit (Bio-Rad, Hercules, CA, USA), and qPCR was performed on total RNA using SsoFast EvaGreen Supermix (Bio-Rad, Hercules, CA, USA), according to the manufacturer's instructions. *GAPDH* was used as the internal control. The relative expression levels were assessed using the following PCR program: 98°C for 2 min; 40 cycles of 98°C for 3 s, 60°C for 10 s, and 95°C for 30 s. Amplification products were analysed via 2% agarose gel electrophoresis. The reverse-transcriptase PCR primers for *CD55* and *GAPDH* were as follows: for the *CD55* fragment, sense: 5′-TTCCCCCAGATGTACCTAATGC-3′, anti-sense: 5′-TTACAGTATCCTCGGGAAAACTTGT-3′; for the *GAPDH* fragment, sense: 5′-GAAGGTGAAGGTCGGAGTC-3′, anti-sense: 5′-GAAGATGGTGATGGGATTTC-3′.

CD55 protein analysis through western blotting analysis

Forty-eight hours post-transfection, the cells were collected with PBS and lysed at 4°C in cell lysis buffer. Equal amounts of samples were loaded onto 12% SDS-polyacrylamide gels for electrophoresis and then transferred to PVDF membranes. The membranes were blocked with 5% skim milk in TBS containing 0.05% Tween 20 at room temperature for 1 h. Membranes were incubated overnight with primary antibodies against CD55 (1:400, ABclonal, Woburn, MA, USA) and β-actin (1:8000, ZenBioScience, Chengdu, China) in 5% non-fat milk at 4°C. After washing the membrane, goat anti-mouse, and anti-rabbit HRP-conjugated secondary antibodies (1:8000, ZenBioScience, Chengdu, China) were used for 2 h. The bands were visualized using a chemiluminescence detection system.

Dual-luciferase reporter assay

The fragment of the 3′-UTR of human *CD55* containing the predicted target site of miR-132-3p (wild-type coding region 3′-UTR) or *CD55* subjected to site-directed mutagenesis of the 3′-UTR (mutant coding region 3′-UTR) was amplified by RT-qPCR. The PCR product was cloned downstream of the modified pmirGlO luciferase reporter vector (GenePharma, Shanghai, China). All constructs were confirmed by DNA sequencing.

For the luciferase assay, 293T cells were seeded into 24-well plates at a density of 1×10^5 cells/well. At 24 h after plating, cells were co-transfected with 50 nM miR-132 mimics or miR-NC mimics and 500 ng of *CD55* 3′-UTR wild-type or CD55 3′-UTR mutant-type plasmids per well using Lipofectamine 2000 (Invitrogen). Luciferase activity was measured 24 h after transfection using the Dual-luciferase Reporter Assay System (Promega, Fitchburg, WI, USA), according to the manufacturer's instructions. For each sample, firefly luciferase activity was normalized to *Renilla* luciferase activity to control for the transfection efficiency.

Complement-mediated cytolysis assay

Cytotoxicity assays were performed using trypan blue exclusion assays, which have been used in many previous studies and are still widely used [18, 32, 36]. Briefly, 48 h after transfection, cells in the logarithmic growth phase were collected from the culture flask using 3 mM EDTA and washed. Cells (1×10^6) from each group were washed and incubated with various dilutions of 50% INHS and NHS (0, 15, 30, and 50%) for 1 h at 37°C. The percentage of dead cells was determined microscopically after mixing the sample with 0.4% trypan blue. The numbers of living and dead cells in each cell suspension sample were counted, and the survival rates were calculated as follows:

Survival rate = living/(dead + living) × 100%, where 'living' = no. of living cells and 'dead' = no. of dead cells.

Fluorescence microscopy

To measure C5b-9/membrane attack complex (MAC) deposition, LoVo-GT and Ls-174T-GT cells were transfected with miR-132-3p mimics or inhibitors and compared with the related negative controls. Forty-eight hours post-transfection, cells (1×10^6) from each group were collected, washed with PBS, and incubated with 50% NHS, for Ls-174T-GT cells, and 15% NHS, for LoVo-GT cells, or INHS at 37°C. After 1 h, the cells were collected with 3 mM EDTA, washed twice, fixed with 4% paraformaldehyde, and incubated with 1% bovine serum albumin (BSA) overnight at 4°C. This was followed by incubation with 100 µl of anti-C5b-9 mAb (dilution 1:200, Abcam, Cambridge, MA, USA), which was diluted with PBS containing 1% BSA for 1 h at 37°C. After washing with PBS, the cells

were incubated with FITC-conjugated goat anti-mouse IgG antibodies (dilution 1:200, Zhongshan Golden Bridge Co., China) for 30 min at room temperature and then incubated with 100 µl of 0.5 µg/ml of DAPI. The cells were then washed to remove the unbound antibodies and DAPI. The cell suspensions (10 µl) were transferred to glass coverslips for confocal microscopy. Cells were imaged under a Leica TCS SP5 confocal microscope. All cells were imaged using the same exposure scaling conditions by applying the same imaging parameters.

C5a ELISA

To measure C5a release (secreted from cells undergoing complement attack), cells (1×10^6) from each group were collected 48 h post-transfection, washed, and incubated with 50% pooled NHS, for Ls-174T-GT cells, and 15% NHS, for LoVo-GT cells, at 37°C. After 30 min, the complement attack was blocked through the addition of EDTA (10 mM final concentration in the supernatant), and the cells were removed via centrifugation at 1500 rpm for 20 min to remove insoluble impurities and cell debris. The cell supernatant was collected and frozen at −80°C until further analysis. C5a levels were determined using a C5a ELISA kit (Elabscience Biotechnology, Wuhan, China). Measurements were performed in triplicate.

Histology and IHC

One of the aliquots was used for haematoxylin and eosin (H&E) staining. The histological diagnosis of all samples was performed and confirmed by experienced pathologists. Tissue samples were inspected to ensure that there was no necrotic tissue, and the tumour cell content was calculated based on the ratio of the tumour area to the normal areas. All specimens were evaluated to ensure that the tumour cell content was at least 70%.

All IHC assays were performed in accordance with the manufacturer's instructions. Briefly, consecutive sections of freshly frozen colon tumour and normal tissue samples were prepared and incubated overnight at 4°C with primary antibodies against CD55 (dilution 1:100; Abcam, Cambridge, MA, USA). The sections were then incubated with the Polink-2 plus Polymer HRP Detection System (Zhongshan Golden Bridge, China). The colour was developed using a diaminobenzidine chromogenic colour development kit (Zhongshan). PBS was used instead of the primary antibody for the negative control group. Normal colon tissue served as the control.

Two independent observers scored all samples in a blinded manner without previous knowledge of the clinicopathologic details of each sample. An immunoreactivity scoring system was applied using the extensional standard as follows: (A) a fraction of positively stained cells of 5% or less was scored as 0 points, 6–25% was scored as 1 point, 26–50% was scored as 2 points, 51–75% was scored as 3 points, and >75% was scored as 4 points; (B) for the intensity of staining, no staining was scored as 0 points, buff was scored as 1 point, yellow was scored as 2 points, and brown was scored as 3 points. The A and B scores were multiplied, and the staining score was stratified as weak (score range, 0–4) or strong (score range, 5–12) according to the proportion and intensity of positively stained cancer cells.

Statistical analysis

Statistical analyses were performed using SPSS 20.0 (IBM, Chicago, IL, USA). Quantitative data were analysed using a two-tailed Student's *t*-test and one-way analysis of variance followed by Dunnett's multiple comparison post-test. Pearson's correlation coefficient was used to measure the statistical relationships between two continuous variables. Results are expressed as the mean ± standard deviation. The differences were statistically significant at $*P < 0.05$, $**P < 0.01$, and $***P < 0.001$.

Results

miR-132-3p expression is down-regulated in high CD55-expressing colon cancer cell line

Bioinformatics tools including TargetScan (http://www.targetscan.org/), DIANAmT (http://diana.imis.athena-innovation.gr/), miRDB (http://www.mirdb.org/), miRWalk (http://zmf.umm.uni-heidelberg.de/), and miRanda (http://www.microrna.org/) were used to determine the candidate miRNAs that target the 3′-UTR of *CD55*. Based on the predicted frequency, we listed the 30 top candidate miRNAs (Table 1) that were proven to be negatively correlated with the malignant phenotype of cancer cell lines or the poor prognosis of patients with cancer in previous studies [25–27]. Our previous study demonstrated that the LoVo cell line expresses very low levels of CD55, whereas the Ls-174T cell line exhibits a high expression of CD55 [18]. We then compared the expression levels of the candidate miRNAs in LoVo and Ls-174T cell lines using RT-qPCR. Expression levels of 12 miRNAs were significantly down-regulated in Ls-174T cells compared to those in LoVo cells (Fig. 1A, Supplementary Table 2). Among these, Ls-174T cells exhibited the lowest expression level of miR-132-3p, relative to that in LoVo cells (1.49 ± 0.74%, $P = 2.15E{-}09$), suggesting that miR-132-3p was the candidate miRNA most likely to target *CD55*, and it was therefore selected for further validation.

miR-132-3p regulates CD55 at the post-transcriptional level

132-3p mimics or inhibitors were transfected into LoVo and Ls-174T cells (Fig. 1B) to determine whether they could alter CD55 expression. RT-qPCR and western blotting assays showed that miR-132-3p mimics significantly reduced the mRNA expression of *CD55* in LoVo cells (21.1 ± 6.66%, $P = 0.00003$) and Ls-174T cells (45.68 ± 15.56%, $P = 0.003$) (Fig. 1C), as well as the protein expression (Fig. 1D) in both cell lines, compared to that with control miRNA mimics (miR-NC). Conversely, the miR-132-3p inhibitor significantly increased CD55 mRNA and protein expression in LoVo cells (3.94 ± 1.03-fold, $P = 0.008$) and Ls-174T cells (2.46 ± 0.73-fold, $P = 0.026$) (Fig. 1C and D). Briefly, miR-132-3p down-regulated the level of CD55 mRNA and protein.

miR-132-3p directly inhibits the expression of CD55 through its 3′-UTR

To verify the direct effects of miR-132-3p on CD55, TargetScan was used to predict the miR-132-3p-binding sequence in *CD55*. As shown in Fig. 1E, the seed sequence of miR-132-3p was complementary to the 3′-UTR of *CD55* from chr1:207359650 to 207359656 (GRCh38.p13 primary assembly). Further, the activity of the luciferase gene, which is downstream of the wild-type CD55 3′-UTR, was decreased with miR-132-3p mimics (68.31 ± 4.92%, $P = 0.0004$), as

Table 1: bioinformatics prediction of miRNAs regulating CD55 expression

Selected miRNAs	Predicted regulatory sites	Selected miRNAs	Predicted regulatory sites
miR-34b-5p	1451-1457 of CD55 3′UTR	miR-421	1205-1211 of CD55 3′UTR
miR-502-5p	93-99 of CD55 3′UTR	miR-335-5p	143-149 of CD55 3′UTR
miR-31-5p	1091-1098 of CD55 3′UTR	miR-19b-3p	543-549 of CD55 3′UTR
miR-132-3p	40-46 of CD55 3′UTR	miR-338-5p	974-981 of CD55 3′UTR
miR-382-5p	157-163 of CD55 3′UTR	miR-200a-3p	1110-1116 of CD55 3′UTR
miR-641	595-601 of CD55 3′UTR	miR-182-5p	1093-1099 of CD55 3′UTR
miR-769-3p	817-823 of CD55 3′UTR	miR-381-3p	7413-7419 of CD55 3′UTR
miR-561-3p	1278-1284 of CD55 3′UTR	miR-203a-3p	2961-2967 of CD55 3′UTR
miR-590-3p	8009-8015 of CD55 3′UTR	miR-186-5p	694-700 of CD55 3′UTR
miR-942-5p	246-252 of CD55 3′UTR	miR-216b-5p	208-214 of CD55 3′UTR
miR-548c-3p	259-265 of CD55 3′UTR	miR-383-5p	7164-7170 of CD55 3′UTR
miR-338-3p	473-479 of CD55 3′UTR	miR-506-3p	2919-2925 of CD55 3′UTR
miR-450b-3p	817-823 of CD55 3′UTR	miR-204-5p	6589-6595 of CD55 3′UTR
miR-578	757-764 of CD55 3′UTR	miR-374a-3p	378-384 of CD55 3′UTR
miR-142-5p	870-876 of CD55 3′UTR	miR-363-3p	4306-4312 of CD55 3′UTR

compared to that with the negative control. However, the miR-132-3p mimics had no effect on luciferase activity from the mutated CD55 3′-UTR reporter (97.31 ± 3.5%, P = 0.25). In other words, the luciferase reporter assay demonstrated that expression of the luciferase gene ligated to the wild-type CD55 3′-UTR, but not the mutated CD55 3′-UTR, was largely reduced by the high expression of miR-132-3p in HEK293T cells (Fig. 1E). Our data suggest that miR-132-3p directly inhibits *CD55* by targeting its 3′-UTR.

miR-132-3p increases the sensitivity of colon cancer cells to antibody-mediated CDC

Strong expression of α-gal was detected in LoVo-GT and Ls-174T-GT cells stably transfected with the α-1,3GT gene by performing direct immunofluorescence (Fig. 2A). Our previous study indicated that transfection with α-gal did not affect cancer cell morphology, growth, and tumourigenesis [18, 28]. Here, the relative expression levels of miR-132-3p in LoVo-GT, Ls-174T-GT, and their parent cell lines were determined by RT-qPCR (Fig. 2B). LoVo and LoVo-GT cells showed similar expression levels of miR-132-3p (P = 0.79), which was also observed for Ls-174T and Ls-174T-GT cells (P = 0.87), indicating that α-gal had no effect on the expression of miR-132-3p.

To determine whether the expression of miR-132-3p would increase the sensitivity of colon cancer cells to antibody-mediated CDC, α-gal-expressing tumour cells were incubated with pooled NHS (concentrations of 15, 30, or 50%) containing both complement- and anti-α-gal-specific antibodies. LoVo-GT and Ls-174T-GT cells were transfected with a miR-132-3p mimic, inhibitor, or negative control. After 48 h, cells were collected and incubated with NHS, and cell death was determined using the trypan blue exclusion assay.

No cytolysis was observed in the two cell lines after incubation with heat-inactivated 50% INHS. However, miR-132-3p mimics significantly enhanced LoVo-GT cell sensitivity to CDC when cells were incubated with 15% NHS compared to that with miR-NC mimics, as the cell viability decreased from 61.35 ± 2.99% to 38.45 ± 1.73% (P = 0.0003). The miR-132-3p inhibitor significantly reduced cell sensitivity to complement-mediated cell death, as compared to that with the miR-NC inhibitor, as cell viability increased from 52.95 ± 5.76% to 70.75 ± 3.05% (P = 0.009). Almost all LoVo-GT cells were killed after incubation with 30 or 50% NHS (Fig. 2C). In Ls-174T-GT cells, which highly express CD55, miR-132-3p mimics only increased cell sensitivity to CDC in the 50% NHS group, with a decrease in cell viability from 94 ± 4.36% to 75.09 ± 4.49% (P = 0.006) (Fig. 2D). No cytolysis was detected in Ls-174T-GT cells incubated with 15 or 30% NHS. These results indicated that the overexpression of miR-132-3p significantly increases α-gal-mediated CDC. Of particular note, this effect was observed in the cell line with low CD55 expression in the presence of low concentrations of NHS and in the cell line with high CD55 expression in the presence of high concentrations of NHS.

miR-132-3p increases complement activation

The ability of miRNAs to regulate CD55 expression suggested the probability that miRNAs regulate C5a release and C5b-9 deposition on targeted cells. LoVo-GT and Ls-174T-GT cells were incubated with NHS, followed by the detection of the MAC. A fluorescence assay was used to test for C5b-9 on the cell surfaces, and an ELISA kit was used to assess the release of C5a in the supernatant. LoVo-GT and Ls-174T-GT cells were transfected with a miR-132-3p mimic, inhibitor, or negative control. miR-132-3p mimics significantly increased the release of C5a in LoVo-GT cells (31.04 ± 3.79 ng/ml vs. 62.93 ± 7.91 ng/ml, P = 0.003) and Ls-174T-GT cells (16.85 ± 1.56 ng/ml vs. 27.9 ± 2.49 ng/ml, P = 0.003) compared to that with miR-NC mimics, whereas the miR-132-3p inhibitor decreased the release of C5a in LoVo-GT cells (27.8 ± 2.01 ng/ml vs. 23.27 ± 1.1 ng/ml, P = 0.026), but not in Ls-174T-GT (15.73 ± 2.6 ng/ml vs. 15.21 ± 1.94 ng/ml, P = 0.79), compared to that with the miR-NC inhibitor (Fig. 3A and B). Additionally, C5b-9 signals were significantly stronger in LoVo-GT cell membranes than in Ls-174T-GT cells. Moreover, miR-132-3p mimics enhanced C5b-9 deposition, whereas the miR-132-3p inhibitor decreased C5b-9 deposition on LoVo-GT cells (Fig. 3C). An increase in C5b-9 deposition in Ls-174T-GT cells was also observed after transfection with miR-132-3p mimics. However, Ls-174T-GT cells transfected with the miR-132-3p inhibitor showed similarly low C5b-9 deposition to that with the miR-NC inhibitor. In brief,

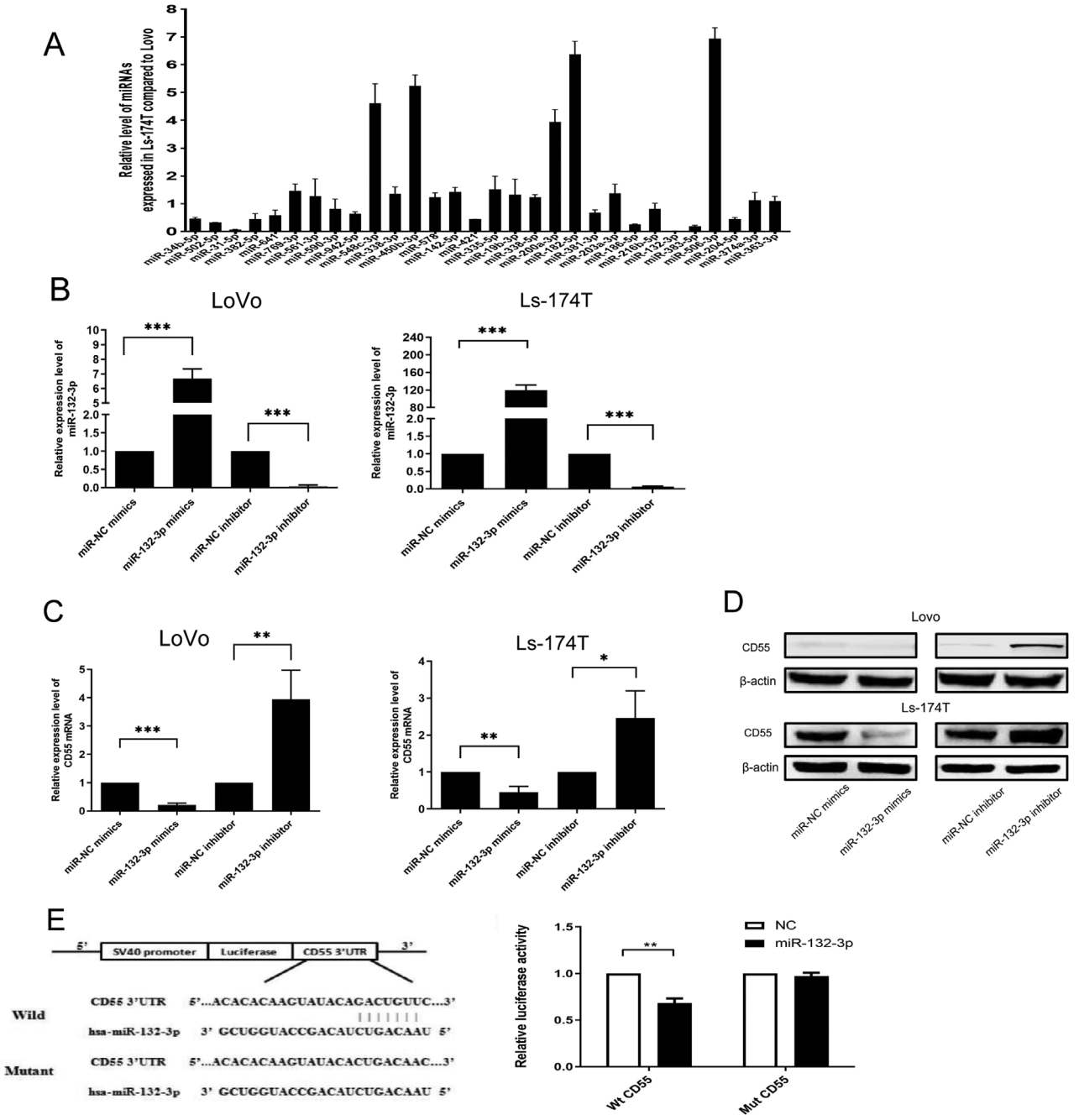

Figure 1: CD55 is a direct target of miR-132-3p. (A) The relative expression level of miRNAs in the Ls-174T cell line was detected by RT-qPCR and compared to the miRNAs levels in the LoVo cell line. (B) miR-132-3p expression level in LoVo or Ls-174T cell lines transfected with the miR-132-3p mimics or inhibitor and their respective negative controls. *CD55* mRNA (C) and protein (D) expression in the LoVo or Ls-174T cell line transfected with the miR-132-3p mimics or inhibitor and their respective negative controls. (E) Schematic representation of the *CD55*-3′-UTR (untranslated region) reporter construct and sequence alignment between miR-132-3p and the *CD55* 3′-UTR wild-type and *CD55* 3′-UTR mutant sequences. Mutations were generated based on the miR-132-3p-binding sequence of the *CD55* 3′-UTR as indicated. Dual-luciferase reporter data with the wild-type and mutated 3′-UTR of *CD55* are shown after miR-132-3p overexpression. **P* < 0.05, ***P* < 0.01, ****P* < 0.001.

miR-132-3p mimics increased C5a release and C5b-9 deposition in both cell lines, but the miR-132-3p inhibitor only decreased C5a release and C5b-9 deposition in LoVo-GT cells.

Expression of miR-132-3p and CD55 in colon tumour tissue

Twenty patients pathologically diagnosed with colon cancer were included, and the proportion of cancer cells in each tumour sample was ≥70% (Fig. 4A and Supplementary Table 1). IHC was used to detect the expression of the CD55 protein, and RT-qPCR was used to detect the expression of *CD55* mRNA and miR-132-3p. IHC showed that the CD55 protein was highly expressed in colon cancer cells compared to that in adjacent normal cells (Fig. 4B). This was confirmed based on the fact that the expression of *CD55* mRNA in tumour tissue was significantly higher than that in normal tissue of the same patient, via a paired *t*-test ($P = 0.0001$). The expression of miR-132-3p in tumour tissues was significantly

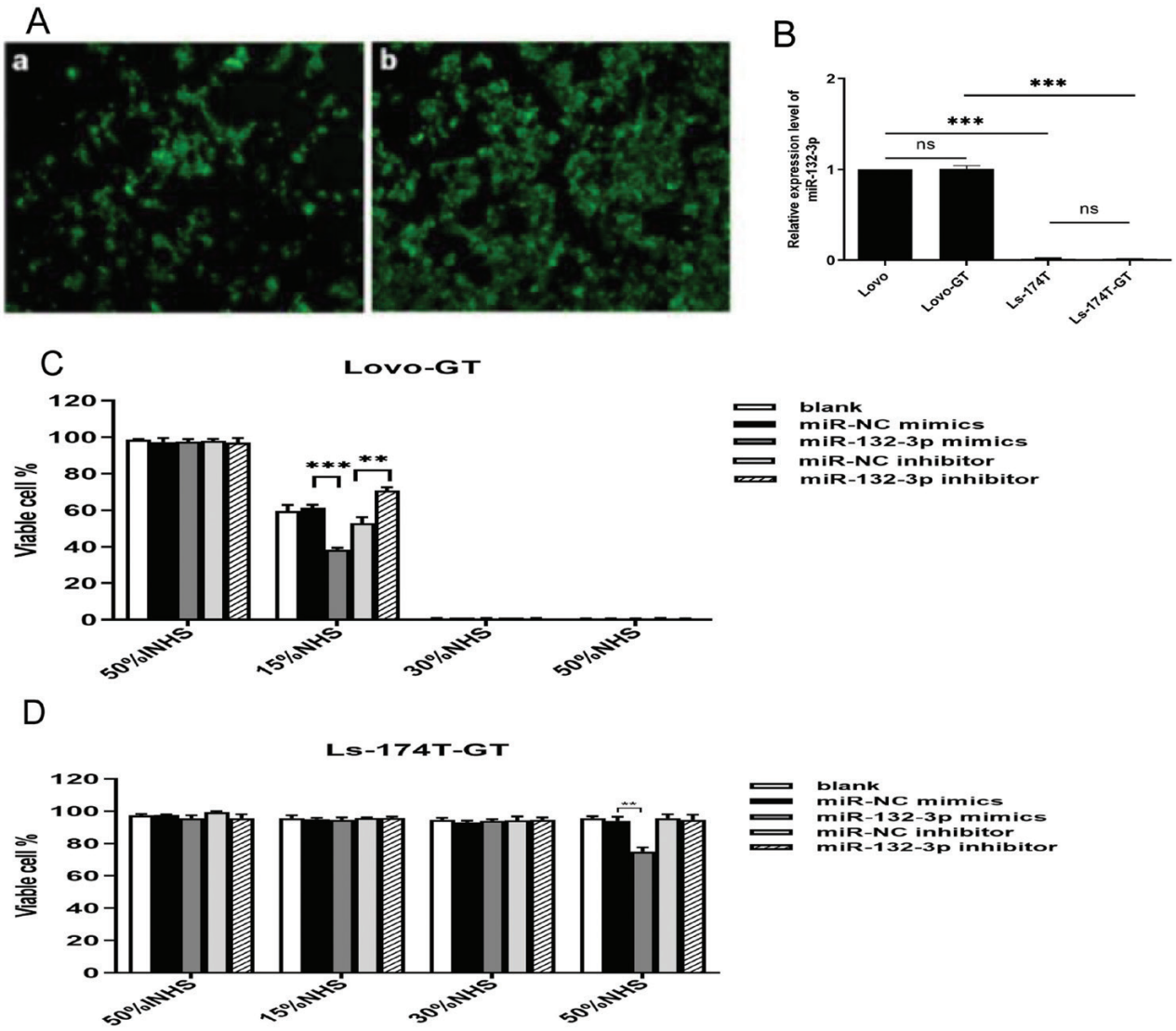

Figure 2: miR-132-3p regulates cell sensitivity to antibody-induced CDC. (A) Expression of the epitope Gala1-3Galb1-4GlcNAc-R (α-gal) on stably transfected LoVo-GT (a) and Ls-174T-GT (b) cells was observed by performing direct immunofluorescence. (B) miR-132-3p expression in LoVo, Ls-174T, LoVo-GT, and Ls-174T-GT cell lines, as detected via RT-qPCR. Survival rates of (C) LoVo-GT and (D) Ls-174T-GT cells transfected with the miR-132-3p mimics and inhibitor or control. All cells were incubated with various dilutions of normal human serum (NHS; 15, 30, or 50%). Error bars show standard deviations. *$P < 0.05$, **$P < 0.01$, ***$P < 0.001$, ns ≥ 0.05.

lower than that in normal tissues of the same patient as determined by performing a paired *t*-test ($P = 0.02$; Fig. 4C). Further, CD55 protein expression was positively correlated with *CD55* mRNA expression ($R = 0.48$, $P = 0.03$) and negatively correlated with miR-132-3p expression ($R = -0.63$, $P = 0.003$) (Fig. 4D). These results indicated that the expression of miR-132-3p is negatively correlated with CD55 expression in colon cancer tissue.

Discussion

Our results for the first time suggest that increasing the level of miR-132-3p potentially down-regulates CD55 mRNA and protein expression at the post-transcriptional level. This results in increased sensitivity to antibody-mediated CDC in colon cancer cell lines via the increased release of C5a and deposition of C5b-9. In colon cancer tissues, miR-132-3p levels are also expressed at lower levels than those in the adjacent normal tissues and are negatively correlated with CD55 protein expression.

Beyond the targeted inhibition of signalling pathways, such as growth factor receptor or angiogenesis pathways, mAbs can also trigger innate immune reactions to cause immune-mediated cell destruction via CDC, which can expand the anti-tumour effect of antibody drugs [29]. Most targeted mAbs can activate the complement system, such as rituximab [30], daratumumab [31], alemtuzumab [32], cetuximab [33], and dinutuximab [34]. However, most tumour cells overexpress mCRPs, including CD46, CD55, and CD59, which can inhibit the mAb-mediated CDC effect, thereby limiting the therapeutic potential of mAbs [10, 13]. Increasing evidence suggests that neutralizing antibodies or siRNAs that down-regulate the expression of mCRPs can significantly enhance mAb-mediated CDC *in vitro* [35]. As a human IgG1 Ab, cetuximab lacks the capacity to activate the complement cascade and cannot trigger sufficient CDC in solid tumours [36,

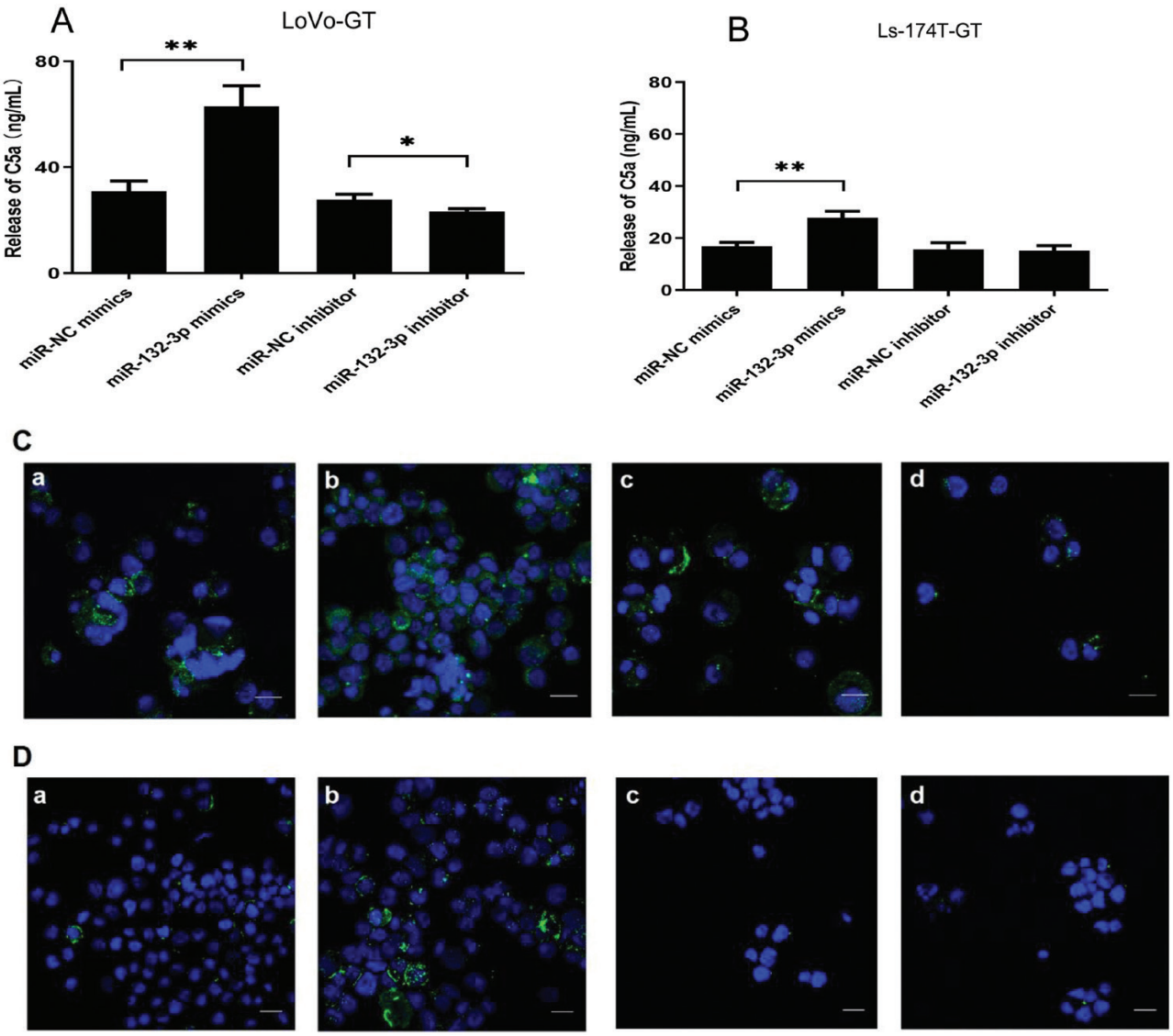

Figure 3: miR-132-3p regulates cell sensitivity to complement activation. The release of (A) C5a from LoVo-GT and (B) Ls-174T-GT cells was detected using an ELISA kit. The deposition of C5b-9 (membrane attack complex; MAC) on (C) LoVo-GT and (D) Ls-174T-GT cells was observed with a fluorescence confocal microscope. LoVo-GT cells were treated with 15% normal human serum (NHS), and Ls-174T-GT cells were treated with 50% NHS. a: miR-NC mimics; b: miR-132-3p mimics; c: miR-NC inhibitor; d: miR-132-3p inhibitor. The bar indicates 20 μm. $^{*}P < 0.05$, $^{**}P < 0.01$.

37]. The single EGFR-specific IgG3 Ab cetuximab triggers significant CDC against CD55-negative or low-expressing target cells, but not CD55-highly expressing cells, as detected using the DiFi colorectal carcinoma cell line [38]. In addition, the inhibition of mCRPs could sensitize leukemic cells or breast cancer cells to CDC upon treatment with rituximab or trastuzumab, respectively [39, 40]. Our previous studies revealed that blocking and down-regulating the expression of CD55 significantly enhances trastuzumab-induced CDC in Her2-positive breast cancer cells [13, 18]. These studies show that the regulation of mCRP expression plays a critical role in the anti-tumour effects of mAbs.

miRNA has shown great potential for the diagnosis and treatment of cancer [41, 42]. Here, we selected miR-132-3p from numerous candidates as one of the potential miRNAs that regulate CD55 in colon cancer cells expressing high and low levels of CD55. miR-132-3p, which is located on human chromosome 17p13.3, has been found to be a tumour suppressor and its expression was determined to be down-regulated in a series of cancers, including breast cancer [43], colorectal cancer [44], hepatocellular carcinoma [45], and lung cancer [46]. Moreover, miR-132 is involved in cell proliferation, migration, and invasion [47]. Nevertheless, the potential mechanisms underlying the involvement of miR-132-3p in the complement-related immune cascade remain unclear. This study extends our understanding of the effects of miR-132-3p on Ab-mediated CDC.

We noticed that miR-132-3p mimics significantly inhibited mRNA and protein of CD55 in Ls-174T-GT cells. However, miR-132-3p mimics had no effect on cell viability of Ls-174T-GT cells in the presence of 15 or 30% NHS. Only a 25% decrease in cell viability was observed in the presence of 50% NHS when cells were transfected with miR-132-3p mimics. One reason is that Ls-174T-GT cells express higher levels of CD59 and CD46, which possibly contribute to the inhibition of Ab-mediated CDC sensitivity [18]. Consistent

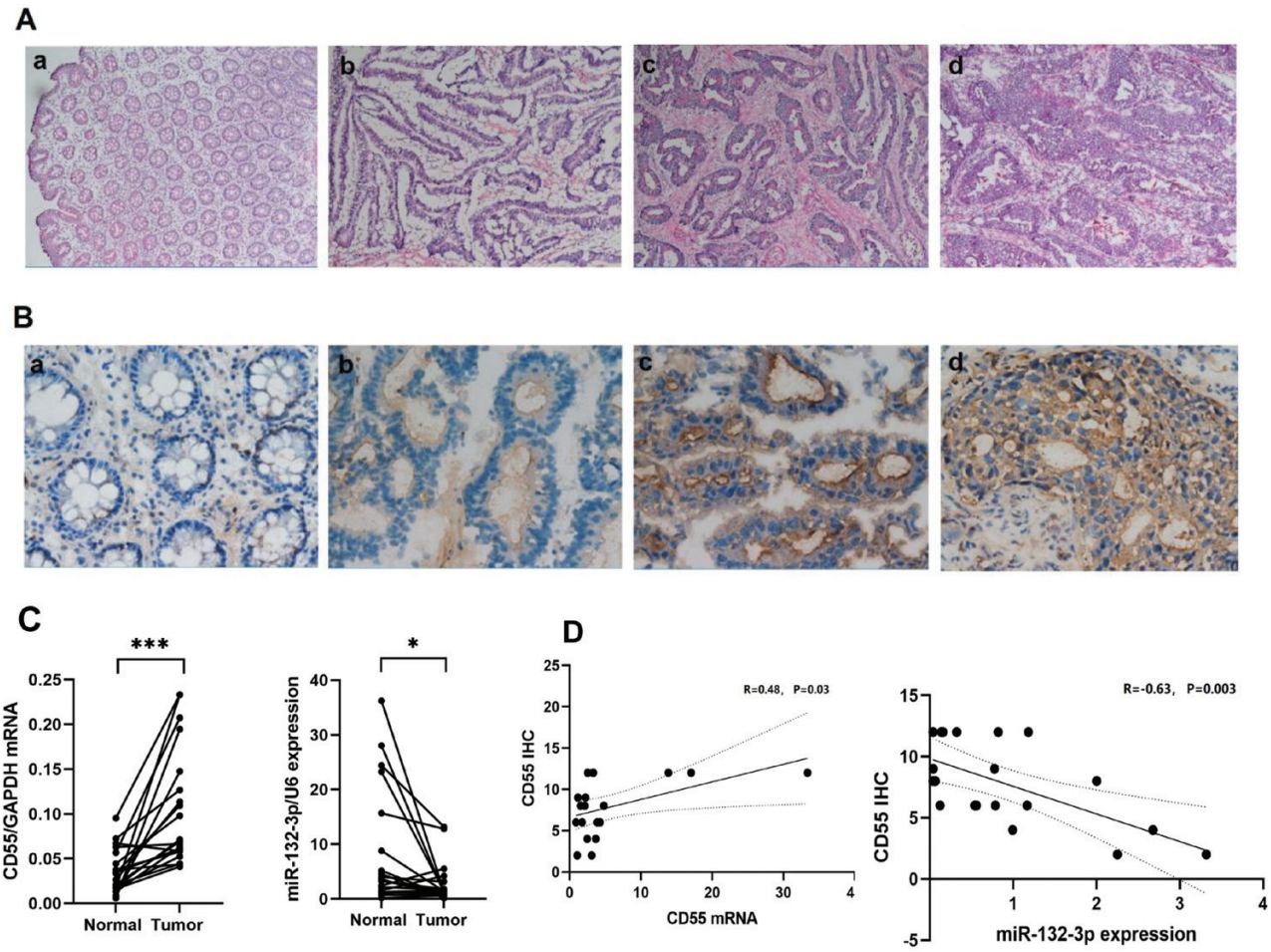

Figure 4: miR-132-3p and CD55 expression level in colon tumour tissues and adjacent normal tissues. (A) H&E staining of frozen tissue samples (×100). (B) Representative images of CD55 expression in human normal colon tissues and colon cancer tissues, as determined through IHC. a: Normal colon tissues. b: Highly differentiated colon cancer tissues. c: Moderately differentiated colon cancer tissues. d: Poorly differentiated colon cancer tissues. (C) Expression of *CD55* mRNA and miR-132-3p in paired tumour tissues and normal tissues. (D) Correlation analysis of CD55 protein based on IHC and *CD55* based on RT-qPCR (left), as well as CD55 protein based on IHC and miR-132-3p based on RT-qPCR. *$P < 0.05$, ***$P < 0.001$.

with *in vitro* experiments, results with colon cancer tissue verified that miR-132-3p was negatively correlated with CD55 expression. However, more colon cancer tissues are needed to explore the relationship between other clinicopathological features and miR-132-3p/CD55 expression. In future sutdy, we need to explore the potiential predictive effect of miR-132-3p and CD55 expression level on antibody drugs efficacy in colon cancer patients who are treated with EGFR-targeting Cetuximab.

Conclusions

We found that miR-132-3p regulates CD55 expression by directly targeting the 3′-UTR of *CD55*, leading to changes in cell sensitivity to Ab-mediated CDC through the release of C5a and deposition of C5b-9. This study provides new evidence for the anti-tumour roles of miR-132-3p and reveals its potential use as a biomarker for the efficacy of antibody drugs that could trigger CDC. We also stress that our in vitro model can be generally applied to explore regulators of Ab-mediated CDC involved in the effects of antibody treatments.

Supplementary data

Supplementary data is available at *Clinical and Experimental Immunology* online.

Ethical approval

This study was approved by the Clinical Test and Biomedical Ethics Committee of West China Hospital Sichuan University (2022(No.684)) for using human tissue specimens and blood samples, and the West China Hospital Ethical Committee granted an exemption from the requirement of consent to use the human tissue specimens. All serum donors signed informed consent forms.

Conflict of interests

The authors declare no competing interests.

Funding

This work was supported by the National Natural Science Foundation of China (grant numbers: 30470762 and 30972940, to Y.P.W.) and the Key research and development

projects of the Science & Technology Department of Sichuan Province (grant number: 2019YFS0342, to Y.F.).

Data availability

The data analysed are included in the main manuscript and Supplementary Tables.

Patient consent statement

Not applicable.

References

1. Scott AM, Wolchok JD, Old LJ. Antibody therapy of cancer. *Nat Rev Cancer* 2012, 12, 278–87. doi:10.1038/nrc3236.
2. Smith MR. Rituximab (monoclonal anti-CD20 antibody): mechanisms of action and resistance. *Oncogene* 2003, 22, 7359–68. doi:10.1038/sj.onc.1206939.
3. Mendelsohn J. Epidermal growth factor receptor inhibition by a monoclonal antibody as anticancer therapy. *Clin Cancer Res* 1997, 3, 2703–7.
4. Hicklin DJ, Witte L, Zhu Z, Liao F, Wu Y, Li Y, et al. Monoclonal antibody strategies to block angiogenesis. *Drug Discov Today* 2001, 6, 517–28. doi:10.1016/s1359-6446(01)01759-7.
5. Kohrt HE, Houot R, Marabelle A, Cho HJ, Osman K, Goldstein M, et al. Combination strategies to enhance antitumor ADCC. *Immunotherapy* 2012, 4, 511–27. doi:10.2217/imt.12.38.
6. Gancz D, Fishelson Z. Cancer resistance to complement-dependent cytotoxicity (CDC): problem-oriented research and development. *Mol Immunol* 2009, 46, 2794–800. doi:10.1016/j.molimm.2009.05.009.
7. Shi Y, Fan X, Deng H, Brezski RJ, Rycyzyn M, Jordan RE, et al. Trastuzumab triggers phagocytic killing of high HER2 cancer cells in vitro and in vivo by interaction with Fcgamma receptors on macrophages. *J Immunol* 2015, 194, 4379–86. doi:10.4049/jimmunol.1402891.
8. Ricklin D, Hajishengallis G, Yang K, Lambris JD. Complement: a key system for immune surveillance and homeostasis. *Nat Immunol* 2010, 11, 785–97. doi:10.1038/ni.1923.
9. Kim DD, Song WC. Membrane complement regulatory proteins. *Clin Immunol* 2006, 118, 127–36.
10. O'Brien RM, Cannon A, Reynolds JV, Lysaght J, Lynam-Lennon N. Complement in tumourigenesis and the response to cancer therapy. *Cancers (Basel)* 2021, 13, 1209.
11. Geller A, Yan J. The role of membrane bound complement regulatory proteins in tumor development and cancer immunotherapy. *Front Immunol* 2019, 10, 1074.
12. Wang Y, Yang YJ, Wang Z, Liao J, Liu M, Zhong XR, et al. CD55 and CD59 expression protects HER2-overexpressing breast cancer cells from trastuzumab-induced complement-dependent cytotoxicity. *Oncol Lett* 2017, 14, 2961–9.
13. Liu M, Yang YJ, Zheng H, Zhong XR, Wang Y, Wang Z, et al. Membrane-bound complement regulatory proteins are prognostic factors of operable breast cancer treated with adjuvant trastuzumab: a retrospective study. *Oncol Rep* 2014, 32, 2619–27. doi:10.3892/or.2014.3496.
14. Galili UA. an abundant human natural antibody of multiple pathogeneses and clinical benefits. *Immunology* 2013, 140, 1–11.
15. Kristian SA, Hwang JH, Hall B, Leire E, Iacomini J, Old R, et al. Retargeting pre-existing human antibodies to a bacterial pathogen with an alpha-Gal conjugated aptamer. *J Mol Med (Berl)* 2015, 93, 619–31.
16. Deguchi T, Tanemura M, Miyoshi E, Nagano H, Machida T, Ohmura Y, et al. Increased immunogenicity of tumor-associated antigen, mucin 1, engineered to express alpha-gal epitopes: a novel approach to immunotherapy in pancreatic cancer. *Cancer Res* 2010, 70, 5259–69. doi:10.1158/0008-5472.can-09-4313.
17. Unfer RC, Hellrung D, Link CJ Jr. Immunity to the alpha(1,3) galactosyl epitope provides protection in mice challenged with colon cancer cells expressing alpha(1,3)galactosyl-transferase: a novel suicide gene for cancer gene therapy. *Cancer Res* 2003, 63, 987–93.
18. Wu Y, Wang Y, Qin F, Wang Z, Wang Y, Yang Y, et al. CD55 limits sensitivity to complement-dependent cytolysis triggered by heterologous expression of alpha-gal xenoantigen in colon tumor cells. *Am J Physiol Gastrointest Liver Physiol* 2014, 306, G1056–64.
19. Yi M, Xu L, Jiao Y, Luo S, Li A, Wu K. The role of cancer-derived microRNAs in cancer immune escape. *J Hematol Oncol* 2020, 13, 25.
20. Si W, Shen J, Zheng H, Fan W. The role and mechanisms of action of microRNAs in cancer drug resistance. *Clin Epigenetics* 2019, 11, 25.
21. Hillman Y, Mazkereth N, Farberov L, Shomron N, Fishelson Z. Regulation of complement-dependent cytotoxicity by microRNAs miR-200b, miR-200c, and miR-217. *J Immunol* 2016, 196, 5156–65. doi:10.4049/jimmunol.1502701.
22. Song G, Song G, Ni H, Gu L, Liu H, Chen B, et al. Deregulated expression of miR-224 and its target gene: CD59 predicts outcome of diffuse large B-cell lymphoma patients treated with R-CHOP. *Curr Cancer Drug Targets* 2014, 14, 659–70. doi:10.2174/1568009614666140818211103.
23. Lu Z, Zhang C, Cui J, Song Q, Wang L, Kang J, et al. Bioinformatic analysis of the membrane cofactor protein CD46 and microRNA expression in hepatocellular carcinoma. *Oncol Rep* 2014, 31, 557–64.
24. Grimson A, Farh KK, Johnston WK, Garrett-Engele P, Lim LP, Bartel DP. MicroRNA targeting specificity in mammals: determinants beyond seed pairing. *Mol Cell* 2007, 27, 91–105. doi:10.1016/j.molcel.2007.06.017.
25. Wang Y, Lin C, Liu Y. Molecular mechanism of miR-34b-5p and RNA binding protein HuR binding to lncRNA OIP5-AS1 in colon cancer cells. *Cancer Gene Ther* 2021, 29, 612–624.
26. Zhang J, Hou L, Liang R, Chen X, Zhang R, Chen W, et al. CircDLST promotes the tumorigenesis and metastasis of gastric cancer by sponging miR-502-5p and activating the NRAS/MEK1/ERK1/2 signaling. *Mol Cancer* 2019, 18, 80.
27. Zhang M, Li Y, Wang H, Yu W, Lin S, Guo J. LncRNA SNHG5 affects cell proliferation, metastasis and migration of colorectal cancer through regulating miR-132-3p/CREB5. *Cancer Biol Ther* 2019, 20, 524–36.
28. Qin F, Zhu SM, Zheng H, Wang Z, Wang Y, Zuo Y, et al. Establishment and identification of human lung adenocarcinoma cell line stably expressing the alpha1, 3-galaetosyltransferase gene from pig. *Sichuan Da Xue Xue Bao Yi Xue Ban* 2010, 41, 194–8, 207.
29. Jin S, Sun Y, Liang X, Gu X, Ning J, Xu Y, et al. Emerging new therapeutic antibody derivatives for cancer treatment. *Signal Transduct Target Ther* 2022, 7, 39.
30. Felberg A, Taszner M, Urban A, Majeranowski A, Jaskula K, Jurkiewicz A, et al. Monitoring of the complement system status in patients with B-cell malignancies treated with rituximab. *Front Immunol* 2020, 11, 584509.
31. Xia C, Ribeiro M, Scott S, Lonial S. Daratumumab: monoclonal antibody therapy to treat multiple myeloma. *Drugs Today (Barc)* 2016, 52, 551–60.
32. Baig NA, Taylor RP, Lindorfer MA, Church AK, Laplant BR, Pavey ES, et al. Complement dependent cytotoxicity in chronic lymphocytic leukemia: ofatumumab enhances alemtuzumab complement dependent cytotoxicity and reveals cells resistant to activated complement. *Leuk Lymphoma* 2012, 53, 2218–27. doi:10.3109/10428194.2012.681657.
33. Holubec L, Polivka J Jr, Safanda M, Karas M, Liska V. The role of cetuximab in the induction of anticancer immune response in colorectal cancer treatment. *Anticancer Res* 2016, 36, 4421–6. doi:10.21873/anticanres.10985.
34. Keyel ME, Reynolds CP. Spotlight on dinutuximab in the treatment of high-risk neuroblastoma: development and place in therapy. *Biologics* 2019, 13, 1–12.

35. Wang B, Yang C, Jin X, Du Q, Wu H, Dall'Acqua W, et al. Regulation of antibody-mediated complement-dependent cytotoxicity by modulating the intrinsic affinity and binding valency of IgG for target antigen. *MAbs* 2020, 12, 1690959.
36. Dechant M, Weisner W, Berger S, Peipp M, Beyer T, Schneider-Merck T, et al. Complement-dependent tumor cell lysis triggered by combinations of epidermal growth factor receptor antibodies. *Cancer Res* 2008, 68, 4998–5003. doi:10.1158/0008-5472.can-07-6226.
37. Klausz K, Berger S, Lammerts van Bueren JJ, Derer S, Lohse S, Dechant M, et al. Complement-mediated tumor-specific cell lysis by antibody combinations targeting epidermal growth factor receptor (EGFR) and its variant III (EGFRvIII). *Cancer Sci* 2011, 102, 1761–8.
38. Rosner T, Lohse S, Peipp M, Valerius T, Derer S. Epidermal growth factor receptor targeting IgG3 triggers complement-mediated lysis of decay-accelerating factor expressing tumor cells through the alternative pathway amplification loop. *J Immunol* 2014, 193, 1485–95. doi:10.4049/jimmunol.1400329.
39. Mamidi S, Hone S, Teufel C, Sellner L, Zenz T, Kirschfink M. Neutralization of membrane complement regulators improves complement-dependent effector functions of therapeutic anticancer antibodies targeting leukemic cells. *Oncoimmunology* 2015, 4, e979688. doi:10.4161/2162402x.2014.979688.
40. Mamidi S, Cinci M, Hasmann M, Fehring V, Kirschfink M. Lipoplex mediated silencing of membrane regulators (CD46, CD55 and CD59) enhances complement-dependent anti-tumor activity of trastuzumab and pertuzumab. *Mol Oncol* 2013, 7, 580–94. doi:10.1016/j.molonc.2013.02.011.
41. Filipow S, Laczmanski L. Blood circulating miRNAs as cancer biomarkers for diagnosis and surgical treatment response. *Front Genet* 2019, 10, 169.
42. Forterre A, Komuro H, Aminova S, Harada M. A comprehensive review of cancer microRNA therapeutic delivery strategies. *Cancers (Basel)* 2020, 12, 1852.
43. Li S, Xu JJ, Zhang QY. MicroRNA-132-3p inhibits tumor malignant progression by regulating lysosomal-associated protein transmembrane 4 beta in breast cancer. *Cancer Sci* 2019, 110, 3098–109. doi:10.1111/cas.14164.
44. Zhang W, Wang Z, Cai G, Huang P. Circ_DOCK1 regulates USP11 through miR-132-3p to control colorectal cancer progression. *World J Surg Oncol* 2021, 19, 67.
45. Huang J, Lu D, Xiang T, Wu X, Ge S, Wang Y, et al. MicroRNA-132-3p regulates cell proliferation, apoptosis, migration and invasion of liver cancer by targeting Sox4. *Oncol Lett* 2020, 19, 3173–80.
46. Su Y, Shetty A, Jiang F. Integrated analysis of miRNAs and DNA methylation identifies miR-132-3p as a tumor suppressor in lung adenocarcinoma. *Thorac Cancer* 2020, 11, 2112–24. doi:10.1111/1759-7714.13497.
47. Rafat M, Moraghebi M, Afsa M, Malekzadeh K. The outstanding role of miR-132-3p in carcinogenesis of solid tumors. *Hum Cell* 2021, 34, 1051–65. doi:10.1007/s13577-021-00544-w.